

Bonding Analysis of Titanocene Borane σ -Complexes

Wai Han Lam and Zhenyang Lin*

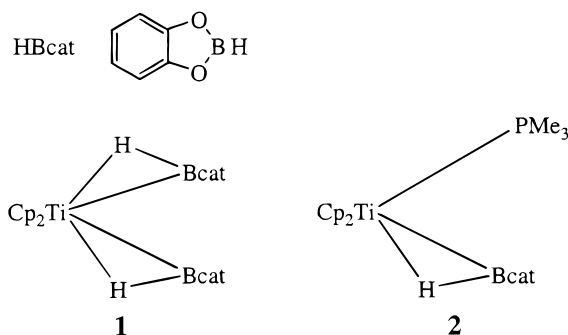
Department of Chemistry, The Hong Kong University of Science and Technology, Clear Water Bay, Kowloon, Hong Kong

Received March 21, 2000

Summary: Bonding analysis has been performed for complexes $\text{Cp}_2\text{Ti}(\eta^2\text{-HBcat})_2$ and $\text{Cp}_2\text{Ti}(\text{PMe}_3)(\eta^2\text{-HBcat})$ through the aid of density functional theory calculations at the level of B3PW91. The significantly short $\text{B}\cdots\text{B}$ contact in the former complex is explained with an unusual three-center–two-electron bond involving the B-Ti-B triangle. In the $\text{Cp}_2\text{Ti}(\text{PMe}_3)(\eta^2\text{-HBcat})$ complex, a related bonding feature involving a metal d orbital and an sp^3 -hybridized fragment orbital derived from the HBcat ligand is found to be responsible for the metal–boron interaction.

Introduction

In an effort to develop efficient and selective catalysts for alkene hydroboration, ^{1–6} Hartwig and co-workers discovered a new and interesting class of titanocene borane σ -complexes containing $\eta^2\text{-H-B}$ ligands.^{7–9} In these complexes (see **1** and **2**), the B-H bond in the



catecholborane acts as a two-electron donor ligand. $\eta^2\text{-B-H}$ coordinations have also been found in many tetrahydroborato transition metal complexes.^{10,11} However, the boron center of the tetrahydroborato ligand in tetrahydroborato complexes is four-coordinated and

achieves the octet. Different from the tetrahydroborato complexes^{10,11} and other σ -complexes,¹² the boron center of the catecholborane ligand in this new class of complexes is three-coordinated and highly electron-deficient in the precoordination state. An interesting structural feature in these complexes is that the coordinated H atom is not coplanar with the $\text{BO}_2\text{C}_6\text{H}_4$ moiety. More surprisingly, the $\text{B}\cdots\text{B}$ distance in the $\text{Cp}_2\text{Ti}(\eta^2\text{-HBcat})_2$ complex **1** is unexpectedly short (2.11 Å) and the B-Ti-B angle is small (53.8°). Clearly, the metal $\eta^2\text{-HBcat}$ bonding feature is very unusual and requires further investigation. The questions raised here are, what is the overall bonding picture for the new class of complexes and is there is a $\text{B}\cdots\text{B}$ bonding interaction in **1**? If yes, what kind of bonding interaction can be described? In this note, we attempt to provide a clearer bonding picture in order to describe the unusual electronic structure and account for the $\text{B}\cdots\text{B}$ bonding interaction with the aid of quantum molecular orbital calculations.

Computational Details

Molecular geometries of model complexes have been optimized using both Becke3LYP¹³ (B3LYP) and Becke3PW91¹⁴ (B3PW91) levels of theory. Geometries obtained from B3PW91 are in better agreement with the experimental ones, and therefore only the results from the B3PW91 calculations are presented here. The Hay and Wadt effective core potentials¹⁵ (ECPs) with a double- ξ valence basis were used to describe the transition metal atom and main-group atoms of period three, while the standard 6-31G basis set¹⁶ was used for all other atoms except for boron and those metal-coordinated hydrogens whose basis sets were augmented by polarization functions ($\xi_p(\text{H}) = 1.0$ and $\xi_d(\text{B}) = 0.6$). To simplify the calculation, model complexes were used in which the Bcat ligand is replaced by $\text{B}(\text{OH})_2$. Previous studies have shown that both DFT and MP2 calculations give comparable accuracy in reproducing experimental structures for transition metal complexes having nonclassical interactions.¹⁷ In view of the size of the systems studied here, DFT methods are used because they require less computational resources.

- (1) (a) Burgess, K.; Ohlmeyer, M. J. *Chem. Rev.* **1991**, *91*, 1179. (b) Irvine, G. J.; Lesley, M. J. G.; Marder, T. B.; Norman, N. C.; Rice, C. R.; Robins, E. G.; Roper, W. R.; Whittell, G. R.; Wright, L. J. *Chem. Rev.* **1998**, *98*, 2685.
- (2) Westcott, S. A.; Blom, H. P.; Marder, T. B.; Thomas Baker, R. J. *Am. Chem. Soc.* **1992**, *114*, 8863.
- (3) Harrison, K. N.; Marks, T. J. *J. Am. Chem. Soc.* **1992**, *114*, 9220.
- (4) Blijpost, E. A.; Duchateau, R.; Teuben, J. H. *J. Mol. Catal. A: Chem.* **1995**, *95*, 121.
- (5) He, X.; Hartwig, J. F. *J. Am. Chem. Soc.* **1996**, *118*, 1696.
- (6) (a) Wade, H. *Angew. Chem., Int. Ed. Engl.* **1997**, *36*, 2441. (b) Braunschweig, H. *Angew. Chem., Int. Ed. Engl.* **1998**, *37*, 1787.
- (7) Hartwig, J. F.; Muhoro, C. N.; He, X.; Eisenstein, O.; Bosque, R.; Maseras, F. *J. Am. Chem. Soc.* **1996**, *118*, 10936.
- (8) Muhoro, C. N.; Hartwig, J. F. *Angew. Chem., Int. Ed. Engl.* **1997**, *36*, 1510.
- (9) Muhoro, C. N.; He, X.; Hartwig, J. F. *J. Am. Chem. Soc.* **1999**, *121*, 5033.
- (10) Marks, T. J.; Kolb, J. R. *Chem. Rev.* **1977**, *77*, 263.
- (11) Xu, Z.; Lin, Z. *Coord. Chem. Rev.* **1996**, *156*, 139.

- (12) Crabtree, R. H. *Angew. Chem., Int. Ed. Engl.* **1993**, *32*, 789.
- (13) (a) Becke, A. D. *Phys. Rev. A* **1988**, *38*, 3098. (b) Miehlich, B.; Savin, A.; Stoll, H.; Preuss, H. *Chem. Phys. Lett.* **1989**, *157*, 200. (c) Lee, C.; Yang, W.; Parr, G. *Phys. Rev. B* **1988**, *37*, 785.
- (14) (a) Burke, K.; Perdew, J. P.; Wang, Y. In *Electronic Density Functional Theory: Recent Progress and New Directions*; Dobson, J. F.; Vinnale, G.; Das, M. P., Eds.; Plenum: New York, 1998. (b) Perdew, J. P.; Burke, K.; Wang, Y. *Phys. Rev. B* **1996**, *54*, 16533.
- (15) Hay, P. J.; Wadt, W. R. *J. Chem. Phys.* **1985**, *82*, 299.
- (16) (a) Gordon, M. S. *Chem. Phys. Lett.* **1980**, *76*, 163. (b) Hariharan, P. C.; Pople, J. A. *Theor. Chim. Acta* **1973**, *28*, 213. (c) Binning, R. C., Jr.; Curtiss, L. A. *J. Comput. Chem.* **1990**, *11*, 1206.
- (17) (a) Fan, M.-F.; Lin, Z. *Organometallics* **1997**, *16*, 494. (b) Choi, S.-H.; Feng, J.; Lin, Z. *Organometallics* **2000**, *19*, 2051.

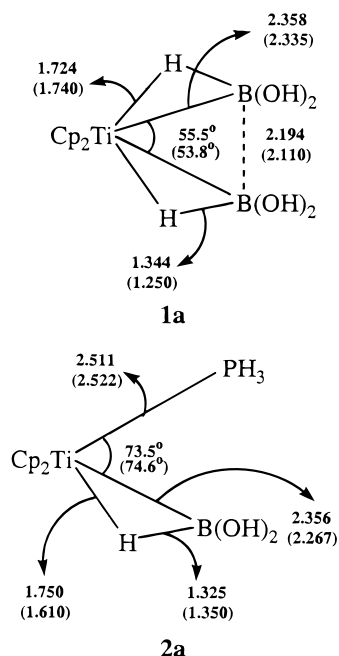


Figure 1. Calculated structural parameters for model complexes $\text{Cp}_2\text{Ti}[\text{HB(OH)}_2]_2$ and $\text{Cp}_2\text{Ti(PMe}_3\text{)}[\text{HB(OH)}_2]$ together with those observed (in parentheses) for complexes $\text{Cp}_2\text{Ti(HBcat)}_2$ and $\text{Cp}_2\text{Ti(PMe}_3\text{)(HBcat)}$.

All calculations were performed using the Gaussian 98 software package¹⁸ on a Silicon Graphics Indigo2 workstation. The electron density analysis was carried out with MOPLOT 2.4,¹⁹ and the charge decomposition analysis (CDA) was done with CDA 2.1.²⁰ The molecular orbitals obtained from the B3PW91 calculations were plotted using the Molden v3.5 program written by G. Schaftenaar.²¹

Result and Discussion

Geometry optimizations were performed for model complexes $\text{Cp}_2\text{Ti}[\eta^2\text{-HB(OH)}_2]_2$ (**1a**) and $\text{Cp}_2\text{Ti(PMe}_3)(\eta^2\text{-HB(OH)}_2)$ (**2a**). HB(OH)_2 and PMe_3 stand for catecholborane and PMe_3 in the complexes whose structures have been actually determined.⁷⁻⁹ The optimized geometries along with the experimentally observed structures are shown in Figure 1. The calculated bond lengths and bond angles are in good agreement with the experimental values. The calculated geometry for **1a** reproduces

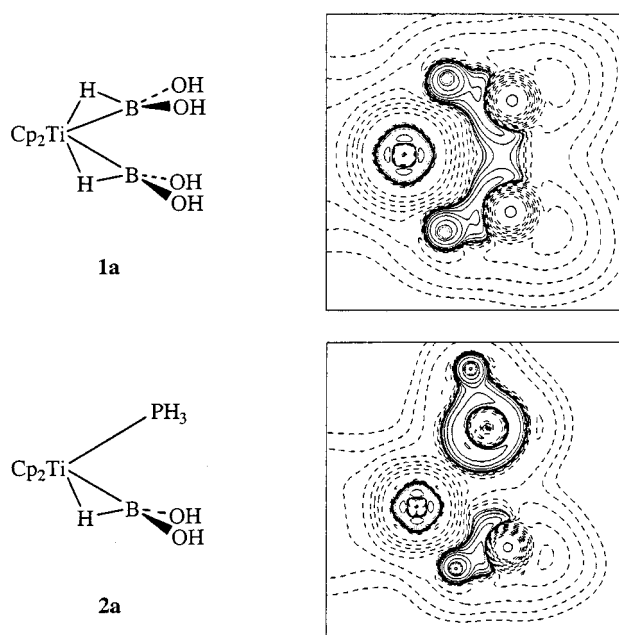


Figure 2. Plots of the Laplacian of electron density for **1a** on the B-Ti-B plane and for **2a** on the B-Ti-P plane.

well the short B...B distance, indicating some form of B...B bonding interaction. The nonplanarity around the boron center of the Bcat ligand for both complexes is also well reproduced. Calculations on the precoordinated ligand, HB(OH)_2 , give B-O and B-H bond distances of 1.364 and 1.190 Å, respectively. These results suggest that in both complexes **1a** and **2a** the back-donation interactions from the metal(d) to the B-H σ^* orbital(s) are significant and the B-H bonds are weakened.

To study the nature of the B...B interaction in $\text{Cp}_2\text{Ti}(\eta^2\text{-HBcat})_2$, we plot the Laplacian of the electron density, $-\nabla^2\rho$, of **1a** in a plane defined by Ti and the two boron atoms (see Figure 2). In the contour plots, solid lines denote $-\nabla^2\rho > 0$, where the electron density is locally concentrated, and dashed lines denote $-\nabla^2\rho < 0$, where the electron density is locally depleted.

Some features of interest in the Laplacian plot can be noted. First, the Ti-H bonds have local concentrations at H and depletions at Ti, indicating a dative bond through the B-H bonds. The four concentrations around the Ti center can be associated with the electron density contributed from a metal d orbital.²² Significant electron density concentrations can be found along the B...B bonding path, suggesting bonding interactions between the two borons. In addition, the B...B bond path is significantly curved inward, with the turning point inclined toward Ti, implying the possibility of a three-center bonding interaction in the B-Ti-B triangle.

On the basis of the results obtained from the Laplacian analysis, a qualitative molecular orbital diagram can be derived (Figure 3) based on the orbital interaction between the Cp_2Ti fragment and the two B(OH)_2 units. It is well-known that the bent metallocene Cp_2Ti fragment has three frontier orbitals available for bonding with additional ligands.²³ These three frontier orbitals are labeled as $1a_1$, b_2 , and $2a_1$, shown in the left column

(18) Frisch, M. J.; Trucks, G. W.; Schlegel, H. B.; Scuseria, G. E.; Robb, M. A.; Cheeseman, J. R.; Zakrzewski, V. G.; Montgomery, J. A., Jr.; Stratmann, R. E.; Burant, J. C.; Dapprich, S.; Millam, J. M.; Daniels, A. D.; Kudin, K. N.; Strain, M. C.; Farkas, O.; Tomasi, J.; Barone, V.; Cossi, M.; Cammi, R.; Mennucci, B.; Pomelli, C.; Adamo, C.; Clifford, S.; Ochterski, J.; Petersson, G. A.; Ayala, P. Y.; Cui, Q.; Morokuma, K.; Malick, D. K.; Rabuck, A. D.; Raghavachari, K.; Foresman, J. B.; Cioslowski, J.; Ortiz, J. V.; Stefanov, B. B.; Liu, G.; Liashenko, A.; Piskorz, P.; Komaromi, I.; Gomperts, R.; Martin, R. L.; Fox, D. J.; Keith, T.; Al-Laham, M. A.; Peng, C. Y.; Nanayakkara, A.; Gonzalez, C.; Challacombe, M.; Gill, P. M. W.; Johnson, B.; Chen, W.; Wong, M. W.; Andres, J. L.; Gonzalez, C.; Head-Gordon, M.; Replogle, E. S.; Pople, J. A. *Gaussian 98 (Revision A.5)*; Gaussian, Inc.: Pittsburgh, PA, 1998.

(19) Interactive MOPLOT: a package for the interactive display and analysis of molecular wave functions, incorporating the programs MOPLOT (D. Lichtenberger), PLOTDEN (R. F. W. Bader, D. J. Kenworthy, P. M. Beddal, G. R. Runtz, and S. G. Anderson), SCHUSS (R. F. W. Bader, G. R. Runtz, S. G. Anderson, and F. W. Biegler-Koenig), and EXTREM (R. F. W. Bader and F. W. Biegler-Koenig) by P. Sherwood and P. J. MacDougall, 1989.

(20) Dapprich, S.; Frenking, G. CDA 2.1; 1994. The program is available via: ftp.chemie.uni-marburg.de/pub/cda.

(21) Schaftenaar, G. Molden v3.5, CAOS/CAMM Center Nijmegen, Toernooiveld, Nijmegen, The Netherlands, 1999.

(22) Fan, M.-F.; Lin, Z. *Organometallics* **1997**, *16*, 494.

(23) Albright, T. A.; Burdett, J. K.; Whangbo, M.-H. *Orbital Interactions in Chemistry*; Wiley: New York, 1985.

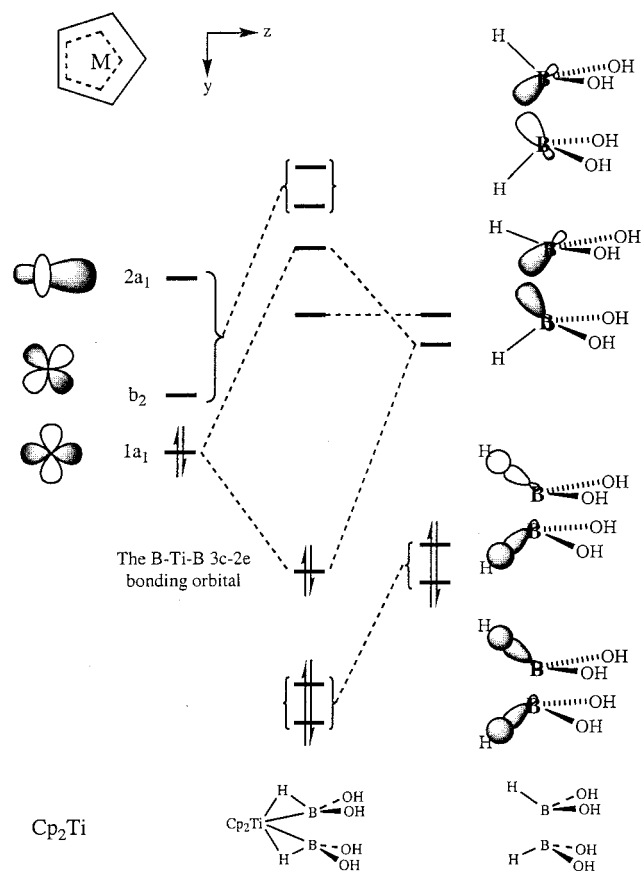


Figure 3. Schematic orbital interaction diagram for the complex **1a**.

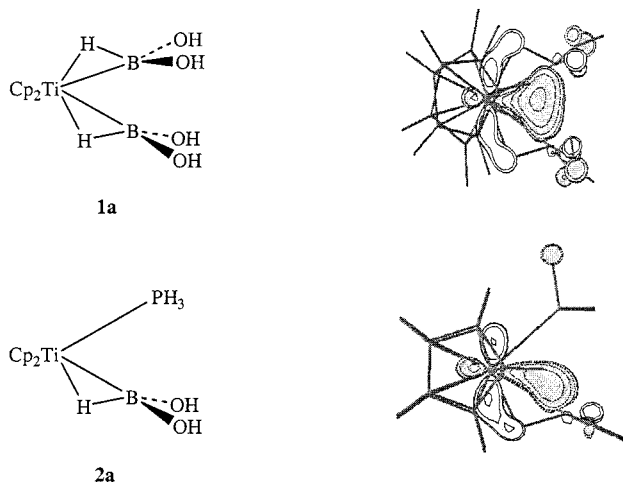


Figure 4. Spatial plots of HOMO for $\text{Cp}_2\text{Ti}[\text{HB}(\text{OH})_2]_2$ (**1a**) and $\text{Cp}_2\text{TiPH}_3[\text{HB}(\text{OH})_2]$ (**2a**).

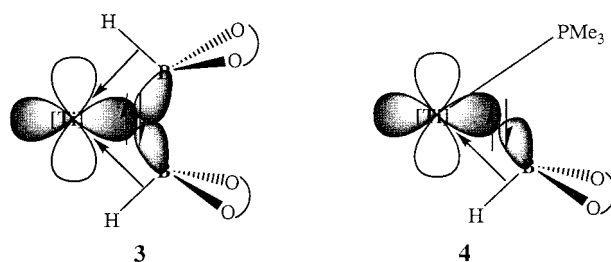
of Figure 3. The corresponding symmetry-adapted ligands' orbitals are derived from the linear combinations of the two B–H bonding orbitals as well as the two empty sp^3 -hybridized orbitals from the two boron centers. These ligands' orbitals are illustrated in the right column of Figure 3. The orbital interactions between the two sets (one from Cp_2Ti and the other from the two $\text{HB}(\text{OH})_2$ units) of orbitals give three bonding and three antibonding orbitals, shown in the central column of Figure 3. A spatial plot (Figure 4) of the highest occupied molecular orbital (HOMO) shows that the major contribution to the HOMO is from the $1a_1$

fragment orbital of Cp_2Ti and the in-phase combination of the two empty sp^3 -hybridized orbitals from the $\text{HB}(\text{OH})_2$ units. This HOMO uniquely forms a three-center–two-electron bond for the $\text{Cp}_2\text{Ti}(\eta^2\text{-HBcat})_2$ complex.

Similarly, the spatial plot (Figure 4) of the HOMO for $\text{Cp}_2\text{Ti}(\text{PH}_3)[\eta^2\text{-HB}(\text{OH})_2]$ again shows the bonding interaction between the $1a_1$ fragment orbital of Cp_2Ti and the empty sp^3 -hybridized orbital from the $\text{HB}(\text{OH})_2$ ligand. Examination of the Laplacian plot (Figure 2) of the $\text{Cp}_2\text{Ti}(\text{PH}_3)[\eta^2\text{-HB}(\text{OH})_2]$ complex shows that the Ti center also has four charge concentrations. A bent Ti–B bonding path can be seen.

Summarizing all the results discussed above, we can intuitively provide schematic bonding models for the two borane σ -complexes studied in this paper (see **3** and **4**).

$[\text{Ti}] = \text{Cp}_2\text{Ti}$



A three-center–two-electron bond is thus used to describe the unique bonding in $\text{Cp}_2\text{Ti}(\eta^2\text{-HBcat})_2$, while a bent bonding interaction is found in $\text{Cp}_2\text{Ti}(\text{PMe}_3)(\eta^2\text{-HBcat})$. These schematic bonding descriptions also find support from our charge decomposition analysis (CDA) calculation. Significant electron flow ($0.427e$ for model complex **1a**) from the $1a_1$ orbital of the Cp_2Ti fragment to the empty orbital(s) of the $\text{HB}(\text{OH})_2$ ligand(s) has been found in the HOMO that forms the three-center–two-electron bond. Similarly, electron flow of $0.284e$ was found for model complex **2a**. The reverse electron flow is also noticeable from the B–H bonding orbital(s) of the $\text{HB}(\text{OH})_2$ ligand(s) to the b_2 and $2a_1$ orbitals of the Cp_2Ti fragment. For model complex **1a**, electron flow of $0.242e$ was found in the two molecular orbitals that represent the bonding in the two Ti–H–B units. For model complex **2a**, electron flow of $0.175e$ was calculated.

It is also of interest to see the effect of lone pairs on the oxygen of the $\text{HB}(\text{OH})_2$ ligand on the 3c–2e bond. Calculation on the hypothetical $\text{Cp}_2\text{Ti}(\eta^2\text{-HBH}_2)_2$ complex shows a much shorter B...B contact (1.926 \AA), indicating that the absence of the lone pairs on substituents at B tends to strengthen the 3c–2e bond.

Conclusion

A three-center–two-electron bond involving the B–Ti–B triangle has been discovered in complex $\text{Cp}_2\text{Ti}(\eta^2\text{-HBcat})_2$. This unusual bonding feature accounts for the experimental observation of the extremely short B...B contact in the complex. The nonplanarity around the B center of the Bcat ligand in the complex leads to an optimal interaction of the 3c–2e bond.

In the $\text{Cp}_2\text{Ti}(\text{PMe}_3)(\eta^2\text{-HBcat})$ complex, a related bonding feature involving a metal d orbital and an sp^3 -hybridized fragment orbital derived from the HBcat ligand is responsible for the metal–boron interaction.

Compared to other σ -complexes, the complexes studied in this paper also have the ligand (σ)-to-metal dative bonds (here ligand (σ) denotes the H–B σ bond of the HBcat ligand) in addition to those unusual bonding characteristics described in this paper.

Acknowledgment. This work was supported by the Research Grants Council of Hong Kong and the Hong Kong University of Science and Technology.

OM000249P